Absorption and extinction correction in quantitative DAFS analysis

Dirk C. Meyer,* Andreas Kupsch and Peter Paufler

TU Dresden, Institut für Kristallographie und Festkörperphysik, D-01062 Dresden, Germany.
E-mail: dirk.meyer@physik.tu-dresden.de

An approach to X-ray attenuation correction for diffraction anomalous fine-structure (DAFS) measurements is presented, taking into account energy-dependent secondary extinction effects. A numerical model based on the kinematical theory of diffraction is presented. This model is exemplified by DAFS measurements of the Zr 0002 reflection intensities for energies in the vicinity of the Zr *K* absorption edge of a Co/Zr multilayer exhibiting strong fibre texture. X-ray absorption fine-structure (XAFS) measurements proved to be a necessary auxiliary for DAFS amplitude correction.

Keywords: DAFS; XAFS; secondary extinction; absorption correction; attenuation correction.

1. Introduction

Quantitative evaluation of diffraction anomalous fine-structure (DAFS; see *e.g.* Stragier *et al.*, 1992) experiments requires energy-dependent attenuation corrections for reflection intensities. The data of mass attenuation coefficients, as tabulated, for example, in the *International Tables for Crystallography* (1999, Vol. C, 2nd ed., ch. 4.2), refer to the common situation where no reflection is excited and include the influences of (true) photoelectric absorption and undirected Rayleigh and Compton scattering of X-rays. We will categorize undirected scattering phenomena under the term 'ordinary' scattering in the following. If a reflection is excited by a suitable wavelength of X-rays and orientation of the lattice planes, a standing-wave field is formed within the sample, *i.e.* scattering and attenuation are related to the direction. Attenuation effects concerning the directed scattered (*i.e.* diffracted) intensities have to be taken into account in the case of strong interference. These additional effects are usually called 'extinction'. In particular, in the case of single crystals and strongly textured material, non-monotonic energy-dependent contributions arising from extinction have to be handled carefully.

Usually two types of extinction are distinguished. *Primary extinction* occurs in crystals consisting of nearly parallel aligned crystallites. These are called 'ideally perfect crystals' and the intensity I_{hkl} is directly proportional to the modulus of the structure factor $|F_{hkl}|$ rather than to $|F_{hkl}|^2$. This reduction of intensity of reflected rays is due to multiple reflections in the uppermost layers. In practice most crystals embody domain sizes such that $I_{hkl} \simeq |F_{hkl}|^n$ ($1 < n < 2$, usually closer to 2). *Secondary extinction* arises because an appreciable portion of the incident ray is reflected by the first crystallite encountered. The crystallites lying beneath receive less incident intensity and thus contribute to the diffracted intensity accordingly less. In the case of small, less well aligned, blocks the crystals are called 'ideally imperfect' (mosaic crystals). For these crystals, secondary extinction can be neglected (*cf.* von Laue, 1960; Stout & Jensen, 1989).

Herein we focus on the influence of secondary extinction for the investigation of single crystals and textured samples for which primary extinction can be neglected ($I_{hkl} \simeq |F_{hkl}|^2$).

Mathematical equations for the evaluation of secondary-extinction effects on integrated intensities have been given by Zachariasen (1963, 1967). These equations are suitable for the cases of perfect and ideal mosaic crystals. For well aligned crystallites, Zachariasen derived an intensity formula that allowed the determination of a mean radius of perfect domains. Zachariasen (1963, 1967) and Tomov & Ivanova (1996) considered a distribution function, with respect to the misalignment of crystallites of a mosaic crystal, that determines the integrated diffracted intensities. A two-order-reflections technique as described by Tomov & Ivanova (1996) allows the evaluation of quantitative parameters for the correction of secondary extinction in the case of mosaic films for which extinction effects are small compared with ordinary attenuation in the non-reflecting case. The idea behind this approach relies on the fact that crystallites contributing to various orders of reflection are the same and thereby have identical pole densities. In the case of films with sharp textures, secondary-extinction effects can even be predominant. To make a solution feasible for that case certain assumptions concerning the distribution functions have to be made.

2. Specimen

The correction formalism will be exemplified by Zr *K* DAFS experiments with a Co/Zr multilayer {[10 × (344 Å Co + 576 Å Zr)] on a Si(001) substrate} prepared by electron-beam vaporization. For details of this system see Kupsch *et al.* (1998). Both types of elemental layers were found to be polycrystalline [*hcp* structure, α-Co, α-Zr, space group (194) ($6_3/mmc$)] and to exhibit a strong [0001] fibre texture (fibre axis parallel to stacking normal). The sample-specific results of the quantitative DAFS and X-ray absorption fine-structure (XAFS) analysis as well as experimental details are described by Meyer, Kupsch *et al.* (1999). Above all, it was the intention of Meyer, Kupsch *et al.* (1999) to pursue thermally stimulated diffusion processes, which may lead to amorphization of crystalline regions, from the point of view of short-range order of the remaining crystallites. The application of DAFS to this sample system was aimed at determining short-range-order structural information of amorphous and polycrystalline volume fractions *separately*. Fluorescence XAFS experiments only enabled an average of the short-range-order information of the sample to be evaluated (see Kupsch *et al.*, 1998). DAFS experiments were carried out in the vicinity of the Zr *K* absorption edge (E_K = 17998 eV) using Zr 0002 reflection intensities measured in a symmetric beam geometry. We recognized that for the present case of strong reflection (corresponding to DAFS conditions) secondary-extinction effects are not negligible. The specimen of the presented investigation corresponds to the as-prepared state, in which the elemental layers occurred separately from each other, *i.e.* the energy-dependent structure factor of the Zr layers was computed as in the ideal structure of α-Zr.

3. Experimental data

In order to determine the attenuation coefficients of the Co/Zr multilayers including energy-dependent fine structure, the Zr *K* DAFS measurements and the Zr *K* fluorescence radiation were detected simultaneously. Measured fluorescence XAFS and Zr *K* DAFS signals are shown in Figs. 1 and 2, respectively. Concerning the computation procedure of the associated energy-dependent absorption coefficients we refer here to the detailed representation of Meyer *et al.* (1998). Values of the densities of the Co and Zr layers were determined experimentally by X-ray reflectometry using multilayers of smaller thickness of the individual (elemental) layers.

 © 2003 International Union of Crystallography • Printed in Great Britain – all rights reserved

Contrary to Zachariasen (1963, 1967) and Tomov & Ivanova (1996), we keep the experimental situation of an excited Bragg reflection for one and the same type of lattice planes and crystallites, respectively, when taking advantage of DAFS intensities of the reflection maximum or integrated intensities. As mentioned above, an appreciable fraction of the incident radiation is reflected by the first crystallites encountered. Thereby the deeper-lying crystallites receive less incident intensity.

Instead of determining absolute reflection intensities, we restricted ourselves to changes in the energy of incident radiation. This restriction, and the fact that diffraction angles have to be varied only slightly for one DAFS scan (typically of the order of 1°), implies, for example, that polarization effects do not change significantly within one experiment thus simplifying the evaluation. On the other hand, in the case of DAFS, we have to start with a completely different approach because of the strong energy dependence of the fine structure of the structure factor.

4. Quantitative DAFS analysis

The theory behind a quantitative DAFS analysis according to Sorensen *et al.* (1994) is based on the approximation of kinematical X-ray diffraction. Therefore, in particular, multiple-scattering processes (primary extinction), multi-beam reflections (Renninger effect) and the attenuation of the electric field by scattering processes (secondary extinction) are neglected.

We present here an approach that allows – in addition to photoelectric absorption and ordinary scattering – the influences of secondary extinction on the DAFS intensities to be handled without the need for a dynamical-scattering formalism.

For a quantitative DAFS analysis, reflection intensities, which are measured as a function of the energy of the radiation, have to be subjected to data reduction as known for ordinary X-ray diffraction experiments (*e.g. International Tables for Crystallography*, 1999, Vol. C, 2nd ed., ch. 4.2). On the pathway inside the sample, absorption and scattering of X-rays give rise to energy-dependent fine structures similar to a transmission XAFS experiment. These oscillating fine structures occur in addition to the effects of resonant corrections $f'(E)$ and $f''(E)$ to the scattering amplitude f. Therefore we need to know the attenuation coefficients (including fine structure) of the sample exactly. One way to obtain exact data of photoelectric absorption coefficients is the simultaneous measurement of fluorescence XAFS of the resonantly scattering element and computation of the associated energy-dependent absorption coefficients by analysis of the measured fluorescence intensities, as described, for example, by Meyer, Gawlitza *et al.* (1999). The attenuation coefficients including the remaining elements of the specimen can then be calculated with an appropriate knowledge of the chemical composition. Another possibility is to accomplish a transmission XAFS measurement. This approach requires dedicated preparation of the sample, particularly regarding a homogeneous thickness, typically of the order of 10 μm. An advantage of such an experiment is that the attenuation coefficient of the sample can be evaluated in a direct way. Also, measurements of the reflection intensities of other crystalline phases occurring in the sample, or of reflections without resonant scattering contributions, can yield the required energy-dependent attenuation coefficients. In order to obtain these coefficients for the case of thin layers the attenuation of substrate reflections penetrating the entire film can be used.

5. Theoretical approach

For the attenuation correction in the geometry of a symmetrical path of X-rays (scattering angle θ) and a flat sample of thickness t (in our case the overall thickness of all Co/Zr layers on the Si substrate) and a total attenuation coefficient $\mu(E)$ (E is the incident energy of X-rays), Sorensen *et al.* (1994) specify the formula

$$A(Q,E) = \{1 - \exp[-2\,\mu(E)\,t/\sin\theta]\}/[2\,\mu(E)/\sin\theta] \qquad (1)$$

for the correction function $A(Q,E)$ (Q represents the magnitude of the scattering vector of the X-rays determined by E and θ). Thereby $A(Q,E)$ is to be applied as a factor to the measured diffracted intensities. Equation (1) is the result of an integration of the scattered intensity contributions $I_s(E)$ of several infinitesimally small scattering elements (located at a depth z from the surface) to the total intensity of one reflection $I(E)$ (Q is held constant for one DAFS scan) over the entire thickness t of the sample,

$$I(E) = \int_0^t I_s(E)\exp[-2\,\mu(E)\,z/\sin\theta]\,dz. \qquad (2)$$

The factor of two in the exponent is inserted because the radiation is attenuated both on the way to the scattering volume fraction and between that point and the detector. For the case of a monotonic device function and looking at the smooth part of the intensities (neglecting the DAFS oscillations) the ratio $U(E)$ of measured intensities $I_m(E)$ to attenuation-corrected theoretical intensities $A(Q,E)\,I_{th}(E)$,

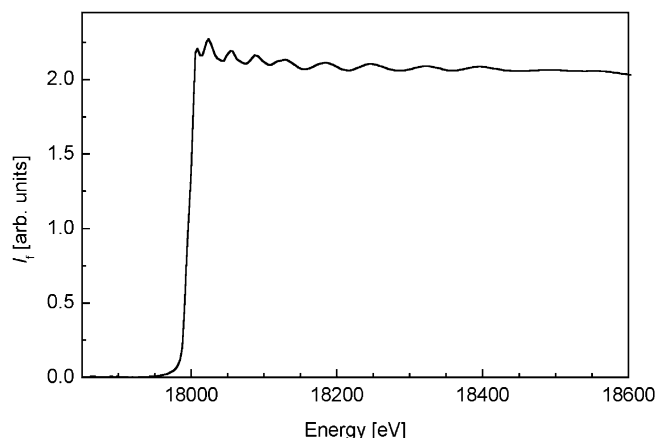

Figure 1
Measured Zr K fluorescence XAFS intensities $I_f(E)$ of the Co/Zr mutilayer.

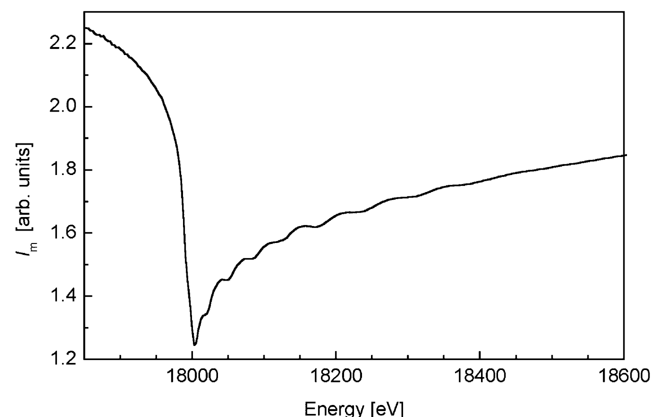

Figure 2
Measured Zr K DAFS intensities $I_m(E)$ of the Zr 0002 reflection of the Co/Zr multilayer.

$$U(E) = I_{\rm m}(E)/[A(Q,E)\,I_{\rm th}(E)], \qquad (3)$$

should show monotonic behaviour as well. Thus the energy dependence of $U(E)$, mainly for energies in the vicinity of the absorption edges, should exhibit no kinks. In the present example of the Co/Zr multilayer the direct application of (1) did not give this result. As already mentioned, it was assumed that for the present specimen (layered structure, strong fibre texture) the secondary extinction is not negligible. In order to be able to go on with the kinematical theory of diffraction it is sometimes useful to consider the impact of the reduction of intensity caused by scattering (Bragg reflection) by increasing the known attenuation coefficient of the sample by multiplication with a factor. However, this approach can be only a general note for certain applications and is not transferable to the specifics of the DAFS analysis.

Our approach is based on the estimation that in the case of strong reflections the intensities are attenuated further. The numerical description outlined below is based on the assumption that the energy dependence of this attenuation is proportional to the square of the modulus of the structure factor F of the reflection and to the path of the X-rays in matter. Therefore the intensities $I_{\rm s}(E)$ scattered by the uppermost lattice planes in the reflection position are prevented from further interaction with the matter lying beneath those planes.

As outlined in the introduction, the choice of the power of two for the structure factor means a restriction to the influence of secondary-extinction effects. If primary extinction cannot be neglected, the power of two can be replaced by a smaller value between 1 and 2. We extend the numerical description of (2) accordingly to

$$I(E) = \int_0^t I_{\rm s}(E)\left\{1 - \left[mz\left|F(E)\right|^2\right]/\sin\theta\right\}\,\exp[-2\,\mu(E)\,z\,/\,\sin\theta]\,{\rm d}z. \qquad (4)$$

Partial integration of (4) yields the extended attenuation function

$$\begin{aligned} A(Q,E) = {} & \left\{1 - \exp[-2\,\mu(E)\,t/\sin\theta]\right\}/[2\,\mu(E)/\sin\theta] \\ & + m|F(E)|^2 t\exp[-2\,\mu(E)t/\sin\theta]/[2\,\mu(E)] \\ & + m|F(E)|^2\sin\theta\{1 - \exp[-2\,\mu(E)\,t/\sin\theta]\}/[4\mu(E)^2]. \qquad (5) \end{aligned}$$

The first additive term agrees with (1) and thus describes the part of the attenuation caused by pure absorption and ordinary scattering. The additional additive terms describe influences of the secondary extinction and are non-vanishing if $|F|^2 \neq 0$.

5.1. Application to the specimen

To apply (5) to the measured DAFS intensities, the sample-specific total absorption coefficients were calculated using the Zr *K* fluorescence signal recorded simultaneously with the DAFS. For extraction of the true photoelectric absorption coefficients including XAFS contributions, the measured Zr *K* fluorescence intensities were corrected for self-absorption effects as outlined, for example, by Meyer, Gawlitza *et al.* (1999). The angle of incidence (which corresponds to the scattering angle θ in the present case) for the Zr *K*-edge DAFS measurements of the Zr 0002 reflection varied between 7° and 9°.

Fig. 3 shows the attenuation correction function $A(Q,E)$ for the Co/Zr multilayer calculated according to (5). The sum of the second and third additive terms of (5) is also plotted in Fig. 3 ($m = 0.007$). It is obvious that the terms connected with secondary extinction contribute to an edge-like attenuation correction function in the vicinity of the absorption edge. For the application of the attenuation correction function to the measured intensities (see Fig. 4), in addition to the energy-dependent reflection intensities, the proportionality factor m [equation (5)] must be determined by evaluating the ratios $U(E)$ for all of the measured intensities. Optimum values for m are those that give a smooth course of $U(E)$ over the entire energy range. This result can be realized *via* a computer program, whereby the values for m can be improved iteratively by reference to appropriate mathematical criteria.

6. Conclusion

We have presented an approach for the correction of secondary extinction in quantitative DAFS analysis. The approach is to be used in experimental situations when the attenuation of the incident and scattered X-rays cannot be described by linear absorption and ordinary scattering solely, but arises due to a considerable fraction from secondary extinction. For practical use we have given an analytical formula for the attenuation correction including those effects applicable for a specimen with planar geometry. The application can be pursued on the example shown for Zr *K* DAFS analysis of a Co/Zr multilayer.

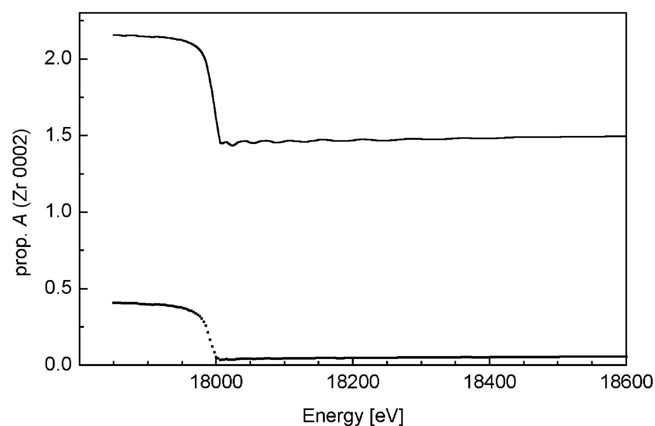

Figure 3
Attenuation correction factors according to (5) for the Co/Zr multilayer (line) and the contribution of the sum of the second and third additive terms ($m = 0.007$) in (5), which describe the attenuation by secondary extinction (dots). The terms considering secondary extinction compared with pure absorption contribute to the overall attenuation factor an extra portion of 23% in the pre-edge region (below 18000 eV) and of 3–4% above the edge.

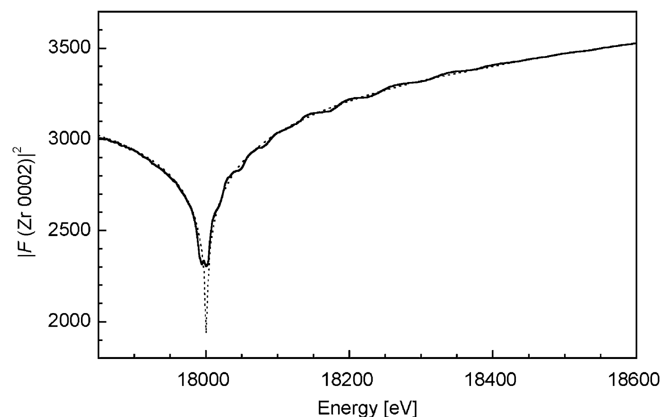

Figure 4
DAFS intensities after application of the attenuation correction function plotted in Fig. 3 (solid line) normalized with respect to theoretical intensities $I_{\rm th}(E)$ (dashes).

The authors thank U. Herr, M. Moske and K. Samwer from Universität Augsburg for supplying the specimens (affiliation according to date of preparation). Moreover, financial support by the DFG and the Fonds der Chemischen Industrie is gratefully acknowledged.

References

Kupsch, A., Meyer, D. C., Richter, K. & Paufler, P. (1998). *J. Alloys Comput.* **266**, 207–215.

Laue, M. von (1960). *Röntgenstrahl-Interferenzen*. Frankfurt am Main: Akademische Verlagsgesellschaft.

Meyer, D. C., Gawlitza, P., Richter, K. & Paufler, P. (1999). *J. Phys. D*, **32**, 3135–3139.

Meyer, D. C., Kupsch, A., Richter, K. & Paufler, P. (1999). *J. Synchrotron Rad.* **6**, 329–331.

Meyer, D. C., Richter, K., Wehner, B. & Paufler, P. (1998). *Philos. Mag. B*, **77**, 891–906.

Sorensen, L. B., Cross, J. O., Newville, M., Ravel, B., Rehr, J. J., Stragier, H., Bouldin, C. E. & Woicik, J. C. (1994). *Resonant Anomalous X-ray Scattering*, edited by G. Materlik, C. J. Sparks & K. Fischer, pp. 389–420. Amsterdam: Elsevier.

Stout, G. H. & Jensen, L. H. (1989). *X-ray Structure Determination*, 2nd ed., pp. 390–394. New York/Chichester/Brisbane/Toronto/Singapore: John Wiley and Sons.

Stragier, H., Cross, J. O., Rehr, J. J., Sorensen, L. B., Bouldin, C. E. & Woicik, J. C. (1992). *Phys. Rev. Lett.* **69**, 3064–3067.

Tomov, I. & Ivanova, K. (1996). *Textures Microstruct.* **26**/**27**, 59–70.

Zachariasen, W. H. (1963). *Acta Cryst.* **16**, 1139–1145.

Zachariasen, W. H. (1967). *Acta Cryst.* **23**, 558–564.

Received 11 June 2002 • Accepted 29 November 2002